Available online at www.sciencedirect.com
SCIENCE DIRECT
Journal of Power Sources 157 (2006) 389–394
JOURNAL OF POWER SOURCES
www.elsevier.com/locate/jpowsour

Short communication

# An algorithm for estimation of membrane water content in PEM fuel cells

Haluk Görgün [a,*], Murat Arcak [b], Frano Barbir [c]

[a] *Yıldız Technical University, Electrical-Electronics Faculty, Istanbul 80750, Turkey*
[b] *Department of Electrical, Computer, and Systems Engineering, 110 8th Street, Rensselaer Polytechnic Institute, Troy, NY 12180, USA*
[c] *Connecticut Global Fuel Cell Center, 44 Weaver Rd. Unit 5233, University of Connecticut, Storrs, CT 06269, USA*

Received 9 May 2005; received in revised form 21 July 2005; accepted 22 July 2005
Available online 12 September 2005

**Abstract**

Available humidity sensing techniques are often intrusive, and of limited practical interest for real-time control applications due to their cost, size, and inadequate response time and accuracy. In this study, we present a novel method for estimation of PEM fuel cell humidity by exploiting its effect on cell resistive voltage drop. This voltage loss is discerned from mass transport, concentration, activation losses and open circuit voltage by a well-known fuel cell voltage model. The proposed scheme makes use of measurements of voltage, current, temperature, and total pressure values in the anode and cathode. It also incorporates dynamic estimators for hydrogen and oxygen partial pressures, adapted from [M. Arcak, H. Gorgun, L.M. Pedersen, S. Varigonda, A nonlinear observer design for fuel cell hydrogen estimation, IEEE Trans. Control Syst. Technol. 12 (1) (2004) 101–110]. The membrane resistance thus obtained is then used to estimate membrane water content following functional characterizations presented in [T.E. Springer, T.A. Zawodzinski, S. Gottesfeld, Polymer electrolyte fuel cell model, J. Electrochem. Soc. 138 (8) (1991) 2334–2342]. Experiments with this estimation technique, performed at the Connecticut Global Fuel Cell Center, are presented and discussed.


*Keywords:* PEM fuel cell; Observer; Estimation; Drying

## 1. Introduction

Polymer electrolyte membrane (PEM) fuel cells are envisioned to be the future choice for portable power, transportation, and combined heat and power systems. They offer advantages to other fuel cell types, including relative simplicity of their design, and their ability to operate at low temperatures. In PEM fuel cells the membrane must be sufficiently hydrated because its conductivity depends critically on the humidity level. Too little water causes membrane drying, which increases the ionic resistance, and exacerbates the voltage drop due to ohmic losses. Too much water causes "flooding", that is blocking of porous passages, which reduces the transport rate of reactants to the catalyst site.

An obstacle to active control of membrane water content is the lack of adequate tools for monitoring humidity in the fuel cell. The cost and size of existing humidity sensors are prohibitive for in situ measurements. Their accuracy is also impaired for high relative humidity levels [3], at which a PEM fuel cell must operate. Other measurement techniques, such as [4] which employs gas chromatography, require extractive sampling and, thus, are slow and intrusive.

In this paper, we present an estimation scheme for the membrane water content. Our idea is to first estimate the membrane resistance and, next, to use available characterizations of membrane resistance as a function of water content, such as those in Ref. [2] for Nafion 112 membranes. To accomplish the first step of membrane resistance estimation we calculate the ohmic voltage loss from voltage and current measurements, and from the well-known fuel cell voltage model [5] which accounts for other voltage loss terms. Because the open-circuit voltage component of this model depends on partial pressures of hydrogen and oxygen, which

* Corresponding author. Tel.: +1 860 486 8762; fax: +1 860 486 8378.
*E-mail addresses:* halukgorgun@alum.rpi.edu (H. Görgün), arcakm@rpi.edu (M. Arcak), fbarbir@engr.uconn.edu (F. Barbir).

0378-7753/$ – see front matter © 2005 Elsevier B.V. All rights reserved.
doi:10.1016/j.jpowsour.2005.07.053

are unavailable for measurement, we estimate them from a variant of the hydrogen and oxygen observers developed in Ref. [1]. We wish to emphasize that our estimation scheme is applicable when the current is nonzero, because it relies on the resistive voltage drop which is induced by the current.

A different approach to humidity estimation is presented in Ref. [6], where the authors employ open-loop observers based on lumped dynamic models for anode and cathode relative humidity values. This approach differs from our voltage-based estimation because, first, it does not make use of the voltage output of the humidity model and, second, it assumes open-circuit conditions. In contrast, we rely on the voltage output and its static relation to water content, and do not employ a dynamic humidity model.

The paper is organized as follows: In Section 2 we review the fuel cell voltage model and the characterization of membrane resistance as a function of its water content. The estimation algorithm is detailed in Section 3, followed by experimental results and their interpretations in Section 4. Remaining research tasks and, in particular, a discussion of how the estimation design can be modified to account for flooding conditions, are presented in Section 5.

## 2. Overview of the voltage model

The theoretical (reversible) voltage of a fuel cell is given by (see e.g. ([5], Chapter 2)):

$$E = -\frac{\Delta \bar{g}_f^0}{2F} + \frac{RT}{2F}\left[\ln\left(\frac{p_{H_2}^{av}}{P_0}\right) + \frac{1}{2}\ln\left(\frac{p_{O_2}^{av}}{P_0}\right)\right] \tag{1}$$

where $\Delta \bar{g}_f^0 < 0$ is the change in molar Gibbs free energy of formation at standard pressure, $P_0$, $R$ the universal gas constant, $F$ the Faraday constant, $T$ the cell temperature, $\ln(\cdot)$ denotes the natural logarithm, and $p_{H_2}^{av}$ and $p_{O_2}^{av}$ represent average values of hydrogen and oxygen partial pressures across the anode and cathode channels, respectively. As discussed in Ref. [1] (Section III), a good approximation for these average values is the arithmetic mean of the inlet and exit partial pressures. However, in some situations the electro-osmotic drag may not be constant along the channel, thus affecting the accuracy of this approximation.

The operational voltage of the fuel cell differs from its theoretical value, $E$; due to the *activation voltage drop*, $V_a$; the *ohmic voltage drop* $V_{ohm}$; the *mass transport loss* $V_{mass}$, as detailed in Ref. [5] (Chapter 3). For a stack of $n$ cells for which the losses are identical, the net voltage is:

$$V_{st} = n(E - V_a - V_{ohm} - V_{mass}). \tag{2}$$

The cumulative effect of the voltage loss terms in (2) is visible from the *polarization curve* in Fig. 1, which gives a plot of the cell voltage as a function of the *current density*; that is, total current $I$ divided by effective membrane area, $A_m$:

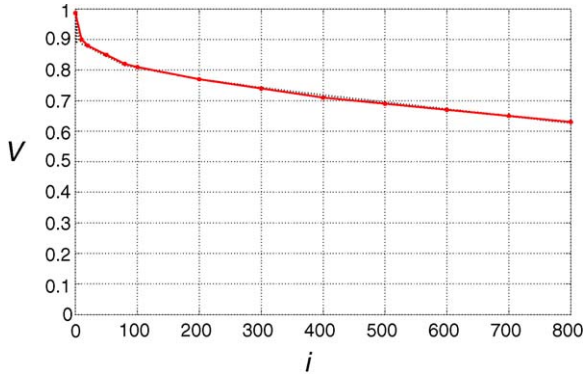


Fig. 1. Voltage of a single cell (V) vs. current density, $i$ (A cm$^{-2}$). The voltage model of Section 2 (continuous curve) matches the discrete data points. Running conditions are: $T_{cell} = 60\,^{\circ}C$, $H_2$ flow = 1 slpm, air flow = 1.5 slpm, humidification temperature = 60 °C.

$$i = \frac{I}{A_m}. \tag{3}$$

Other voltage losses due to fuel crossover and internal currents ([5], Section 3.5) are not included in (2) because their effect is considerable only at very low current densities.

The activation voltage drop is the voltage lost in driving the chemical reactions on the surface of the electrodes. It is given by the well-known empirical formula ([5], Section 3.4):

$$V_a = \frac{RT}{2\alpha F}\ln\left(\frac{i}{i_0}\right) \quad i > i_0, \tag{4}$$

where $\alpha$ is the charge transfer coefficient, and $i_0$ is the exchange current density, which depends on the temperature, pressure, the type of catalyst and its specific surface area and loading [7]. Likewise, the mass transfer voltage drop is given by ([5], Section 3.7):

$$V_{mass} = -B\ln\left(1 - \frac{i}{i_{lim}}\right) \quad i < i_{lim}, \tag{5}$$

where $B$ is a constant that depends on the fuel cell, and its operating conditions and $i_{lim}$ is the *limiting current density*, estimated from experimental data.

Finally, the ohmic voltage drop is

$$V_{ohm} = (R_m + r)I, \tag{6}$$

where $R_m$ is the membrane resistance, and $r$ represents the sum of other components, such as resistance through electrically conductive components of the fuel cell, including contact resistance, and resistance from the electrodes. Because measurement techniques are available to distinguish between the components of total resistance [8], for our design in the next section we assume that $r$ is known.

The membrane resistance, $R_m$, depends critically on the membrane *water content*, which is defined as the ratio of the number of water molecules to the number of charge sites. Indeed, as shown in Ref. [2], water content affects the mem-

brane resistance via

$$R_m = \frac{t_m}{A_m(0.00514\lambda_m - 0.00326)} \times \exp\left[1268\left(\frac{1}{T} - \frac{1}{303}\right)\right] \quad (7)$$

where $t_m$ and $A_m$ are the membrane thickness, and area, respectively. The study in Ref. [2] also relates the membrane water content to the *relative humidity*, $\phi_m$ (the ratio of water partial pressure to saturated vapor pressure) that the membrane is exposed to by the empirical formula:

$$\lambda_m = 0.043 + 17.81\phi_m - 39.85\phi_m^2 + 36.0\phi_m^3. \quad (8)$$

## 3. Estimation of water content

To estimate the water content, $\lambda_m$, our approach is to first estimate $R_m$ and, next, to invert the function (7) to obtain the estimate $\hat{\lambda}_m$. For the estimation of $R_m$ we rely on (6), in which $I$ is available for measurement and $r$ is known. Because $V_{ohm}$ is not measured separately, it is to be calculated from the measurement of the net voltage $V_{st}$, by substituting in (2) the values of $E$, $V_a$, and $V_{mass}$, calculated from (1), (4), and (5), respectively.

This algorithm should not be applied for zero or small values of the current $I$, because the computation of $R_m$ from (6) involves division by $I$. It is reliable when the fuel cell operates in the linear region of the polarization curve because, then, the effect of humidity on the open-circuit voltage, not modeled in (1), and losses due to fuel crossover and internal currents, not accounted for in (2), are indeed negligible compared to the ohmic voltage drop. Since the linear region of the polarization curve is the desired regime of fuel cell operation, this restriction does not impair the practical relevance of our algorithm.

The main difficulty in this algorithm is the calculation of the open-circuit voltage, $E$, from (1), which relies on the unmeasured hydrogen and oxygen partial pressures, $p_{H_2}^{av}$ and $p_{O_2}^{av}$. To overcome this difficulty we employ a variant of the hydrogen and oxygen observer developed in Ref. [1]. To this end we denote by $p_{H_2}$ the exit partial pressure of hydrogen in the anode channel and obtain, from the Ideal Gas Law, the lumped dynamic model [9]:

$$\dot{p}_{H_2} = \frac{RT}{Vol_a}\left(\frac{1}{M_{ai}}\frac{p_{H_{2in}}}{P_{ain}}F_{ai} - \frac{1}{M_{ao}}\frac{p_{H_2}}{P_a}F_{ao} - \frac{nI}{2F}\right) \quad (9)$$

where $\dot{p}_{H_2}$ denotes the time derivative of $p_{H_2}$. $Vol_a$ is the anode volume, $P_a$ the total anode pressure, $p_{H_{2in}}$ and $P_{ain}$, respectively, the hydrogen partial pressure and the total pressure at the inlet of the anode, $F_{ai}$ and $F_{ao}$ the total inlet and outlet mass flows, and $M_{ai}$ and $M_{ao}$ represent average molecular weights of the inlet and exit gas streams. The bracketed expression in (9) calculates the molar rate of change of hydrogen. In particular, the first term represents the increase in hydrogen mole number due to the inlet flow, the second term is the decrease due to the exit flow, and the third term is the consumption due to the fuel cell reaction.

For observer design we assume that the total pressures $P_{ain}$ and $P_a$, and the mass flows $F_{ai}$ and $F_{ao}$, are known. The mass flows can either be measured with flow meters, or estimated from pressure differences via orifice equations, such as those used in Ref. [1]. The variables $M_{ai}$ and $p_{H_{2in}}$ which appear in the coefficient of $F_{ai}$ in (9) are also assumed to be available. This assumption is meaningful when the gas composition of the inlet stream is known, or estimated with a separate observer for the fuel reformer as in Ref. [10]. Our observer mimics Eq. (9) and produces an estimate, $\hat{p}_{H_2}$, for the exit partial pressure $p_{H_2}$ from:

$$\dot{\hat{p}}_{H_2} = \frac{RT}{Vol_a}\left(\frac{1}{M_{ai}}\frac{p_{H_{2in}}}{P_{ain}}F_{ai} - \frac{1}{\hat{M}_{ao}}\frac{\hat{p}_{H_2}}{P_a}F_{ao} - \frac{nI}{2F}\right). \quad (10)$$

For the unknown $M_{ao}$, we employ the value

$$\hat{M}_{ao} = \frac{\hat{p}_{H_2}}{P_a}M_{H_2} + \frac{P_a - \hat{p}_{H_2}}{P_a}\delta_a, \quad (11)$$

in which $M_{H_2}$ is the molecular weight of hydrogen, and $\delta_a$ is an average value for the molecular weights of other gases at the anode exit. If pure hydrogen is supplied to the anode, $\hat{M}_{ao}$ must be taken to be $M_{H_2}$. Unlike the design in Ref. [1] which employed a constant average value for $\hat{M}_{ao}$, the new observer (10) and (11) is nonlinear in $\hat{p}_{H_2}$ due to the dependence of $\hat{M}_{ao}$ on $\hat{p}_{H_2}$. However, because hydrogen is lighter than the other molecules; that is, $M_{H_2} < \delta_a$ in (11), the right-hand side of (10) is a monotone decreasing function of $\hat{p}_{H_2}$, which guarantees observer convergence as proven in Ref. [11].

Using a similar model for the cathode, and denoting by $\hat{p}_{O_2}$ the estimate of $p_{O_2}$ we obtain the oxygen observer

$$\dot{\hat{p}}_{O_2} = \frac{RT}{Vol_c}\left(\frac{1}{M_{ci}}\frac{p_{O_{2in}}}{P_{cin}}F_{ci} - \frac{1}{\hat{M}_{co}}\frac{\hat{p}_{O_2}}{P_c}F_{co} - \frac{nI}{4F}\right) \quad (12)$$

$$\hat{M}_{co} = \frac{\hat{p}_{O_2}}{P_c}M_{O_2} + \frac{P_c - \hat{p}_{O_2}}{P_c}\delta_c, \quad (13)$$

where $Vol_c$ is the cathode volume, $P_c$ the total cathode pressure, $p_{O_{2\,in}}$ and $P_{cin}$ the oxygen partial pressure and the total pressure at the inlet of the cathode, $F_{ci}$ and $F_{co}$ the total inlet and outlet mass flows, $M_{ci}$ and $M_{co}$ represent average molecular weights of the inlet and exit gas streams, $M_{O_2}$ the molecular weight of oxygen and $\delta_c$ is an average value for the molecular weights of other gases in the exit stream.

To estimate the membrane water content $\lambda_m$, we first estimate the theoretical voltage $E$ by obtaining $\hat{p}_{H_2}$ and $\hat{p}_{O_2}$ from the observers (10), (11) and (12), (13), and by substituting in (1) the average values:

$$p_{H_2}^{av} = \frac{\hat{p}_{H_2} + p_{H_{2in}}}{2} \qquad p_{O_2}^{av} = \frac{\hat{p}_{O_2} + p_{O_{2in}}}{2}. \quad (14)$$

Next, we calculate $V_{ohm}$ from (2), using our estimate of $E$, as well as the measurement of voltage $V_{st}$, and the calculation of $V_a$ and $V_{mass}$ from (4) and (5). We then obtain the

membrane resistance estimate $\hat{R}_m$ from (6) by using the current measurement $I$, and by subtracting $r$. Finally, we use this $\hat{R}_m$ to estimate the water content $\hat{\lambda}_m$ from (7), and obtain $\hat{\phi}_m$ from the unique real root of the polynomial (8), given by:

$$\hat{\phi}_m = 0.369 + (S + \sqrt{Q^3 + S^2})^{1/3} + (S - \sqrt{Q^3 + S^2})^{1/3} \quad (15)$$

where $S = -0.0416 + \hat{\lambda}_m/72$ and $Q = 0.0288$.

## 4. Experimental results

We now present experimental results for the algorithm developed in the previous section. These experiments have been performed at the Connecticut Global Fuel Cell Center, with Fuel Cell Technologies Inc. hardware and a 3 M membrane electrode assembly. The active area is $A_m = 50\,cm^2$, and the membrane thickness is $t_m = 0.0051$ cm. Both anode and cathode flow channels are four path serpentine. Hydrogen and air are supplied from hydrogen and air cylinders. Hydrogen and air flows are regulated and humidified by a Teledyne Medusa RD fuel cell test station. A Scribner Associates 890C electronic load bank is used to generate the load current profile. The cell resistance is measured by the current interrupt technique which is integrated to the load bank and controlled by software.

We first compare the voltage model of Section 2 to the experimental polarization curve. To obtain this curve we set the hydrogen flow rate to 1 standard liter per minute (slpm), and the air flow rate to 1.5 slpm. The hydrogen and air humidification temperatures were set to 60 °C. To prevent condensation, we set the line-heaters for hydrogen and oxygen to 70 °C. We observed the open circuit voltage for each cell, then gradually increased the current up to 40 A (800 mA $cm^{-2}$ at $H_2$ stoichiometry around 3), and reduced it back to zero. The resulting curve is given in Fig. 1, where the discrete data points are obtained from step changes in the current every 3 min. We obtained a close match to these data points using the voltage model of Section 2 (continuous curve in Fig. 1) with $B = RT/2F$ and $i_{lim} = 1.4\,A\,cm^{-2}$ in (5), $\alpha = 0.5$ in (4), and with $i_0$ obtained from a temperature- and pressure-dependent formula in Ref. [7], in which we used the reference value $i_0^{ref} = 3.4 \times 10^{-11}\,A\,cm^{-2}$, resulting in apparent exchange current density of $i_0 = 8.8 \times 10^{-8}\,A\,cm^{-2}$.

To test our humidity estimation algorithm, we induced membrane drying by increasing the cell temperature above the humidification temperature. Specifically, the cell temperature was raised from 60 to 80 °C while the humidifier temperature was kept at 60 °C. This causes the air to absorb water from the membrane as it passes through the warmer cell. The resulting increase in the resistance and the decrease in the cell voltage are shown in Fig. 2 for a current of 40 A. Due to the absence of humidity measurements in our set-up, in this paper we compare our estimate $\hat{R}_m$ for the membrane

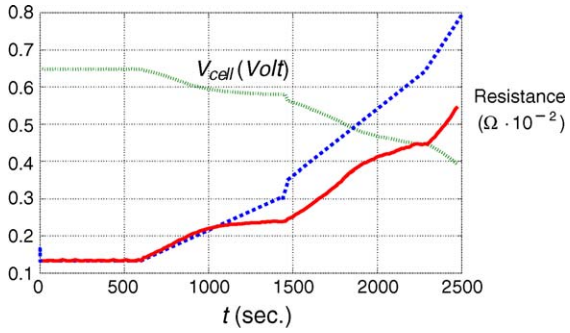


Fig. 2. Voltage decrease and resistance ($\times 10^{-2}\,\Omega$) increase in response to drying, which starts at $t = 600$ s. Solid line is the measured resistance and the dashed line is the sum of our estimate $\hat{R}_m$, and $r = 0.344\,m\Omega$.

resistance to that obtained from the current interrupt measurement in Fig. 2. The observer calculations are presently carried out off-line, from filtered experimental data.

At fully humidified conditions the cell performance was in steady state and the resistance measurement indicated 1.33 mΩ (65 mΩ $cm^2$), as shown in Fig. 2. The model (7) predicts the membrane resistance to be $R_m = 0.986\,m\Omega$ (49 mΩ $cm^2$), which means $r = 1.33–0.986 = 0.344\,m\Omega$ (17 mΩ $cm^2$). 10 mΩ $cm^2$ of this may be attributed to the resistance from the electrodes [12]. Therefore, the electronic resistance is 7 mΩ $cm^2$, which includes the resistance through the electrically conductive components of the fuel cell. In Ref. [13], the electronic resistance is reported to be up to three times larger than the ionic resistance (membrane and electrodes). This, of course, depends on the cell design.

Under drying, the cell resistance increased at a rate of 0.0018 mΩ $s^{-1}$. The electronic resistance should be fairly independent of the drying conditions, i.e., membrane water content. Although drying of the membrane results in reduced thickness, in a well designed fuel cell stack, the changes in the membrane thickness should be compensated by a stack compression mechanism. It is therefore safe to assume that only the ionic resistance changes with humidity in the cell.

The resulting observer estimate of $R_m$ derived from the observance of the cell stack potential, upon addition of $r = 0.344\,m\Omega$ is shown with a dotted curve in Fig. 2. It achieves reasonable accuracy with respect to the measured resistance (solid curve). After $t = 1000$ s, however, it overestimates the measured values. This is due to other factors affecting the cell potential under drying conditions, such as the loss of active sites. Indeed, it is reported in Ref. [14] that drying of the anode catalyst layer not only increased the membrane proton-conduction resistance but also increased the activation overpotential for the hydrogen oxidation reaction due to a decrease in the number of active sites on the anode side. A similar argument may be applied to the cathode drying scenario, where the loss of active sites results in a change of apparent exchange current density. In our experiment, the apparent exchange current density changed from $i_0 = 8.8 \times 10^{-8}\,A\,cm^{-2}$ at 60 °C with fully humidified reactant gases to $i_0 = 1.01 \times 10^{-8}\,A\,cm^{-2}$ at 80 °C with dry gases,

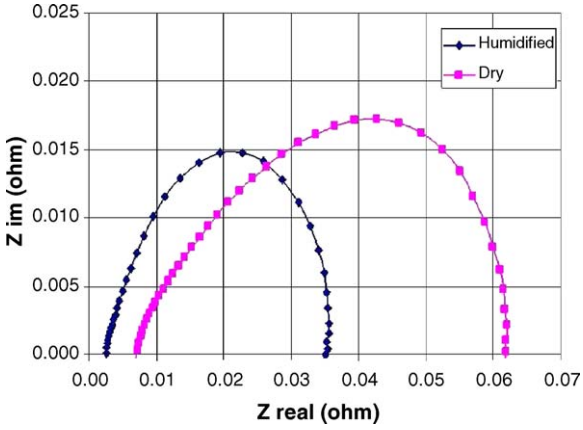


Fig. 3. Impedance spectroscopy of the cell under humidified, and dry conditions.

which corresponds to about 60 times lower active catalyst surface area.

This explanation is corroborated by impedance spectroscopy results in Fig. 3 where the left lobe corresponds to humid conditions (100% relative humidity) while the right lobe corresponds to dry conditions (40%). The measurements were collected over a frequency range of 0.1 Hz to 10 kHz with amplitude of 10 mV using a Solartron Inc. electrochemical interface and frequency response analyzer. The left intersection with the real axis is the high frequency measurement, which represents membrane, contact and electronic resistances, while the right intersection, low frequency measurement, includes charge transfer resistance in addition. Under drying conditions the left intersection moves to the right indicating an increase in membrane resistance. The width of the lobe, however, also increases which means that the charge transfer resistance has also increased.

We wish to emphasize, however, that the main interest in our estimation algorithm is for use in a feedback controller that regulates the humidity around 100% and, thus, the accuracy achieved within the first 1100 s in Fig. 2 is satisfactory for appropriate control action to be taken.

Using the estimated $\hat{R}_m$ in Fig. 2, we obtain from Eqs. (7) and (15) the estimates, $\hat{\lambda}_m$ and $\hat{\phi}_m$, as in Fig. 4. It is clear

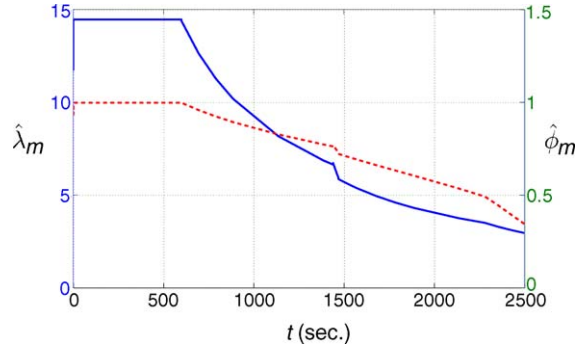


Fig. 4. Water content estimate $\hat{\lambda}_m$ (solid line), and relative humidity estimate $\hat{\phi}_m$ (dashed line), scaled by 10, obtained via Eqs. (7) and (15) from the estimate $\hat{R}_m$ in Fig. 2.

that the membrane was intensively drying with $\hat{\lambda}_m$ dropping below 4. Relative humidity of the gases, once they reach the stack operating temperature, was changing from 100% at cell temperature of 60 °C, to 64% at 70 °C, to 42% at 80 °C. Corresponding relative humidities at the stack outlet (both anode and cathode) were 100% at both 60 and 70 °C, while at 80 °C it was 69%. The average relative humidity of the gases at 80 °C was about 50%, which is also confirmed in Fig. 4.

Note that the experiments above do not include flooding conditions which would also cause a voltage drop at constant current. To distinguish between flooding and drying, a cathode pressure drop may be monitored [15] and incorporated in our algorithm. Pressure drop on the cathode side increases with cell flooding, while it remains unchanged with cell drying, thus clearly distinguishing between the two phenomena [15–17]. Further details on the use of cathode pressure drop as a diagnostic signal may be found in Ref. [15], and is not repeated here.

## 5. Conclusions

Water management is an important problem for PEM fuel cell operation. In this paper a method for estimation of membrane water content has been developed by exploiting its effect on cell resistive voltage drop. This method relies on measurements of voltage, current, temperature, and total pressure in the anode and cathode. It also incorporates observers for hydrogen and oxygen partial pressures adapted from Ref. [1].

A voltage drop at constant current may also be caused by flooding—an effect completely opposite from drying. In order to avoid an incorrect attribution of this voltage drop to drying, a cathode pressure drop may be monitored [15] and incorporated in our algorithm. Pressure drop on the cathode side increases with cell flooding, while it remains unchanged with cell drying, thus clearly distinguishing between the two phenomena [15–17].

Dry conditions at the cell inlet and outlet mean that all of the water generated in the electrochemical reaction evaporated, unlike in steady state saturated conditions at cathode inlet and outlet when all of the product water left the stack as liquid. The Gibbs free energy, and therefore the theoretical cell potential, are lower for gaseous product water. Additional effects of water evaporation on local temperature, and therefore on saturation conditions, may only be determined by detailed 3D modeling, and then integrated over the entire cell.

An additional effect of cell drying on activation overpotential has been detected in experiments. This effect can be compensated for in our algorithm upon further modeling efforts for the increase of activation overpotential relative to the increase in purely resistive voltage drop. Compensation for the additional voltage losses brought on by time (MEA degradation, poisoning, etc.) would be possible with further diagnostic tools that indirectly detect such losses.

## Acknowledgements

The authors would like to thank Dr. Alevtina Smirnova of the Connecticut Global Fuel Cell Center for her help in interpreting experimental results. The work of the second author was supported by NSF under grant ECS-0238268.

## References

[1] M. Arcak, H. Gorgun, L.M. Pedersen, S. Varigonda, A nonlinear observer design for fuel cell hydrogen estimation, IEEE Trans. Control Syst. Technol. 12 (1) (2004) 101–110.
[2] T.E. Springer, T.A. Zawodzinski, S. Gottesfeld, Polymer electrolyte fuel cell model, J. Electrochem. Soc. 138 (8) (1991) 2334–2342.
[3] R.S. Glass (Ed.), Sensor Needs and Requirements for Proton-Exchange Membrane Fuel Cell Systems and Direct-Injection Engines, Lawrence Livermore National Laboratory, Applied Energy Technologies Program, Livermore, California, 2000.
[4] M.M. Mench, Q.L. Dong, C.Y. Wang, In situ water distribution measurements in a polymer electrolyte fuel cell, J. Power Sources 124 (2003) 90–98.
[5] J. Larminie, A. Dicks, Fuel Cell Systems Explained, second ed., John Wiley & Sons Inc., Chicester, 2003.
[6] D. McKay, A. Stefanopoulou, Parametrization and validation of a lumped parameter diffusion model for fuel cell stack membrane humidity estimation, in: Proceedings of the 2004 American Control Conference, Boston, MA, 2004, pp. 816–821.
[7] H.A. Gasteiger, W. Gu, R. Makharia, M.F. Mathias, Tutorial: catalyst utilization and mass transfer limitations in the polymer electrolyte fuel cell, in: The 2003 Electrochemical Society Meeting, Orlando, FL, 2003.
[8] M. Smith, D. Johnson, L. Scribner, Electrical test methods for evaluating fuel cell MEA resistance, Fuel Cell Mag. (February/March) (2004) 15–17.
[9] J. Pukrushpan, A.G. Stefanopoulou, H. Peng, Control of Fuel Cell Power Systems: Principles, Modeling, Analysis and Feedback Design (Advances in Industrial Control), Springer, 2004.
[10] H. Gorgun, M. Arcak, S. Varigonda, S. Bortoff, Nonlinear observer design for fuel processing reactors in fuel cell power systems, in: Proceedings of the 2004 American Control Conference, Boston, MA, 2004, pp. 845–849.
[11] M. Arcak, P. Kokotović, Nonlinear observers: a circle criterion design and robustness analysis, Automatica 37 (12) (2001) 1923–1930.
[12] F.N. Buchi, G.G. Scherer, Investigation of the transversal water profile in nafion membranes in polymer electrolyte fuel cell, J. Electrochem. Soc. 148 (3) (2001) A183–A188.
[13] F. Barbir, J. Braun, J. Neutzler, Effect of collector plate resistance on fuel cell stack performance, in: S. Gottesfeld, T.F. Fuller (Eds.), Proton Conduction Membrane Fuel Cells II, vol. 98-27, The Electrochemical Society, Pennington, NJ, 1999, pp. 400–406.
[14] B. Andreaus, A.J. McEvoy, G.G. Scherer, Analysis of performance losses in polymer electrolyte fuel cells at high current densities by impedance spectroscopy, Electrochim. Acta 47 (2002) 2223–2229.
[15] F. Barbir, H. Gorgun, X. Wang, Relationship between pressure drop and cell resistance as a diagnostic tool for PEM fuel cells, J. Power Sources 141 (1) (2005) 96–101.
[16] F. Barbir, A. Husar, V. Venkataraman, Pressure drop as a diagnostic tool for PEM fuel cells, in: The 2001 Electrochemical Society Meeting, San Francisco, CA, 2001.
[17] W. He, G. Lin, T.V. Nguyen, Diagnostic tool to detect electrode flooding in proton exchange membrane fuel cells, AIChE J. 49 (12) (2003) 3221–3228.